

Aerodynamic investigations on a helicopter fuselage with rotor hub

F. Vogel, C. Breitsamter and N.A. Adams

Institute of Aerodynamics

Technische Universität München

Germany

ABSTRACT

The focus of this investigation is on the flow around a helicopter fuselage with rotor hub. The shape of the wind tunnel model which is used for the experimental studies is based on a light-transport-helicopter with conventional rotor. The model is equipped with a powered main rotor hub. The results include force measurements with an internal six-component balance and velocity measurements with hot-wire anemometry. The aerodynamic forces and moments acting on the helicopter depend strongly on the variation of angle of attack and sideslip. The empennage, which is mounted on the helicopters tail and provides the helicopter with aerodynamic stability in forward flight, is partially responsible for this dependence.

The wake of the fuselage and rotor hub consists of different vortices, generated at different positions on the helicopter fuselage. The structure of these vortices changes with variation of the angle of attack.

NOMENCLATURE

C_D	drag coefficient
C_Y	sideforce coefficient
C_L	lift coefficient
C_l	rolling moment coefficient
C_m	pitching moment coefficient
C_n	yawing moment coefficient
C_p	pressure coefficient
D	drag
L	lift

R	blade radius
Re	Reynolds number
l_{ref}	reference length
S_{ref}	reference area
u	streamwise velocity component
V_∞	freestream velocity
x,y,z	streamwise, spanwise and transverse coordinate directions
α	angle of attack
β	angle of sideslip
Ω	rotational frequency of rotor
ω_x	X component of vorticity
μ	advance ratio
PIV	Particle Image Velocimetry
RPM	rounds per minute

1. INTRODUCTION

The flow around a helicopter fuselage-tail configuration has a very complex topology. Due to flow separation different kind of vortices are generated at specific regions on the fuselage.

Generally, a helicopter fuselage is a blunt body, which does not possess aerodynamic stability under usual flight conditions for disturbances with respect to the change of the angle of the incident flow. An empennage mounted on the tailboom of the helicopter provides the helicopter with stability. However, over the wide angle-of-attack range and sideslip range the flow around the helicopter varies strongly, and also the wake of the fuselage is affected by this variation. Besides the variation of forces and moments caused by the changing incidence of the flow, there is also an apparent influence of the fuselage and the rotor hub wake on the empennage system.

For analysing this necessary stability over a wide range of angle of attack and also for a range of sideslip angles, it is important to investigate the variations of forces and moments and the reason for those variations over such a wide range. A high number of investigations have been carried out previously to quantify the forces and moments on a helicopter fuselage [2, 3, 4], but for a small range of angle of attack and sideslip only. The focus for that work was drag reduction of the helicopter fuselage.

In the present work the flow around a helicopter fuselage with tailboom and rotor hub is investigated over a wide angle-of-attack range and sideslip to obtain more information on the behaviour of the aerodynamic forces and moments on the helicopter with these conditions. Also the changing wake structures due to the variation of angle of attack and the influence of the powered rotor hub are investigated.

2. EXPERIMENTAL SETUP

The helicopter model used for the experimental investigations in the wind tunnel is a 1:7.333 scale model of a light transport helicopter (Fig. 1).

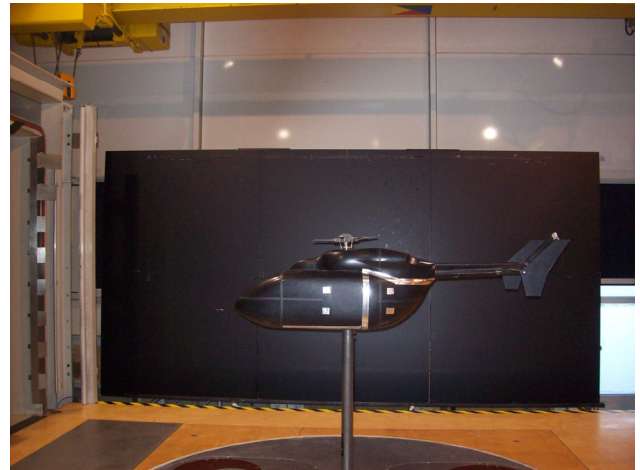


Fig. 1: Helicopter model in wind-tunnel

It consists of the fuselage with the engine canopy, the tail with an empennage, the tail rotor mount (without the rotor) and the model frame, in which the force measurement system and the pitch angle adjustment, is integrated. The model is mounted on a strut in the wind tunnel test section

The pitch-angle adjustment allows for the rotation of the model around a defined axis (Fig. 2) in the range of $\alpha = \pm 40^\circ$. The mechanism for the rotation of the model consists of a shaft assembly. All the necessary components are mounted on the rotating frame. It is powered by a stepping motor placed in the fuselage. The adjustment of the sideslip angle is accomplished by a rotating plate which is integrated in the wind-tunnel floor. The strut of the helicopter is mounted on that rotating plate. The variation of the sideslip angle is possible over a range of $\beta = 0^\circ - \pm 180^\circ$.

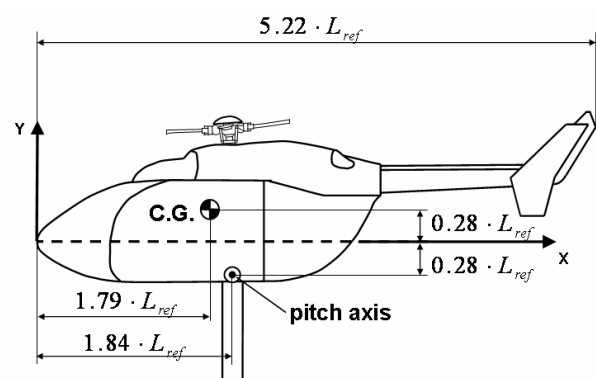


Fig. 2: Dimensions of wind-tunnel model

The model can be equipped with a powered rotor hub which is shown in Fig. 3. It is also possible to use the model without rotor and closed engine canopy (Fig. 4). The rotor hub is powered by an electric servo engine.



Fig. 3: Engine canopy with rotor hub



Fig. 4: Engine canopy without rotor hub

The rotating speed of the hub is adapted to the freestream velocity of the model based on the advance ratio $\mu=0.315$ which is defined according to equation (1). The rotation of the rotor hub is based on the coordinate system in Fig. 2 and turns in positive direction. The rotor hub consists of the rotor mast, the hub fairing, the swashplate, the four rods for blade angle control and the four blade segments.

$$\mu = \frac{V_{\infty}}{\Omega \cdot R} \quad (1)$$

Free stream velocity V_{∞} [m/s]	Re_{ref} [-]	RPM [1/min]
25	$0.528 \cdot 10^6$	1010
30	$0.633 \cdot 10^6$	1212
40	$0.844 \cdot 10^6$	1617

Table 1: Rotating speeds of the rotor hub for different free stream velocities

For the force measurements there is an internal six component balance available, which is placed in the helicopter fuselage. The front part of the balance is mounted with the helicopter model and the rear part is attached to the rotating frame with the strut, so that all aerodynamic forces and moments acting on the helicopter are captured by the balance without the forces acting on the strut. The balance is a six-component strain gauge balance. The six measured signals of the balance are transmitted by cables over the strut to the testing bridge. The measurement system is fully computer controlled. The velocity field is measured by a hot-wire anemometry. The four-wire probe is moved by a 3-axes traversing system in the wake of the helicopter fuselage (Fig. 5). The spacing of the measurement points is 10 mm. The anemometer output is low-pass filtered at 1000 Hz and the sampling rate is 3000 Hz over 6.4 seconds.



Fig. 5: Velocity measurement setup

3. RESULTS AND DISCUSSION

3.1 Force measurements

The force measurements are conducted at a free stream velocity of 40 m/s ($Re_{ref}=0.84 \times 10^6$) for the angle-of-attack variation and 30 m/s ($Re_{ref}=0.63 \times 10^6$) for sideslip-angle variation. The angle-of-attack range was $\alpha = \pm 40^\circ$ with increments of $\Delta\alpha = 2.5^\circ$ and for sideslip-angle range $\beta=0^\circ - 180^\circ$ with increments of $\Delta\beta = 10^\circ$. Two different configurations have been measured:

- Fuselage, tailboom with empennage, powered rotor hub
- Fuselage, tailboom without empennage, powered rotor hub

The force and moment coefficients are defined according to the coordinate system shown in Fig. 2, and the origin of the moment coefficients is the centre of gravity. For the angle-of-attack variation and the sideslip variation the forces and moments are transferred into the wind-tunnel fixed coordinate system.

The force measurements were performed in the wind-tunnel facility A of the Institute of Aerodynamics (AER) at the Technische Universität München (TUM). The wind-tunnel has an open test section with the length of 4.8 m, a width of 2.4 m and a height of 1.8 m. The turbulence level at the nozzle exit is less than 0.4%.

3.1.1 General behaviour of aerodynamic forces and moments

The basic helicopter configuration which is considered here is the fuselage, the tail with the empennage and the powered rotor hub. The pitching-moment coefficient as a function of the angle of attack shows (Fig. 6) that there is

a broad range $\alpha=-12^\circ$ to $\alpha=10^\circ$, in which a stabilizing moment exists. This can be explained by the lift production by the horizontal stabilizers of the empennage. The horizontal stabilizers consists of two airfoil segments to produce a negative lift at $\alpha=0^\circ$. The effective range of the horizontal stabilizers is limited by the flow separation on the airfoil sections. The separation occurs for positive angle of attacks earlier than for negative angles, due to the asymmetric shape of the airfoil. As can be seen from Fig. 6 the maximum achievable pitching moment is for negative angle of attack larger than for the positive ones. Also the fuselage wake can be responsible for an earlier separation.

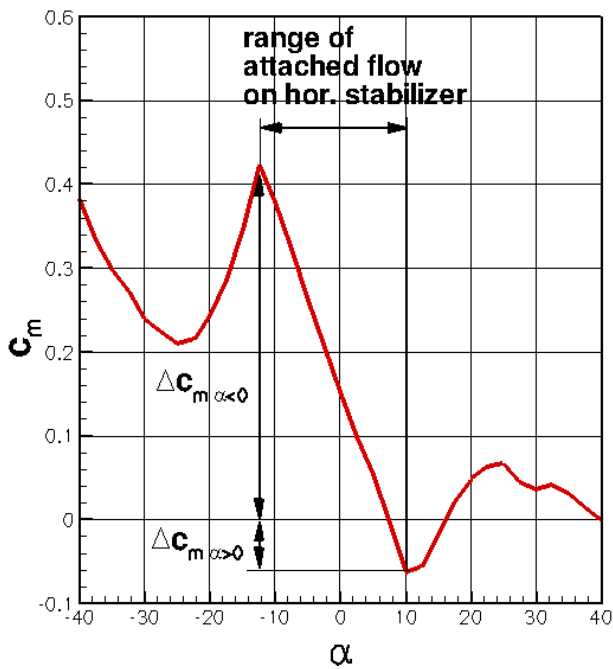


Fig. 6: Pitching moment coefficient as function of angle of attack ($\beta=0^\circ$)

The vertical stabilizers and the tail rotor mount provide the helicopter with a positive yaw moment for a usual forward-flight condition at $\alpha=0^\circ$ and $\beta=0^\circ$ (Fig. 7). This moment supports the anti torque effect of the tail rotor in forward flight and give the helicopter the possibility for safe landing after a loss of the tail rotor.

The tendency of the yaw moment to grow to very high negative values, by increasing sideslip angle, is also caused by the vertical stabilizers. This change in the yaw moment leads to a stabilizing effect for sideslip disturbances.

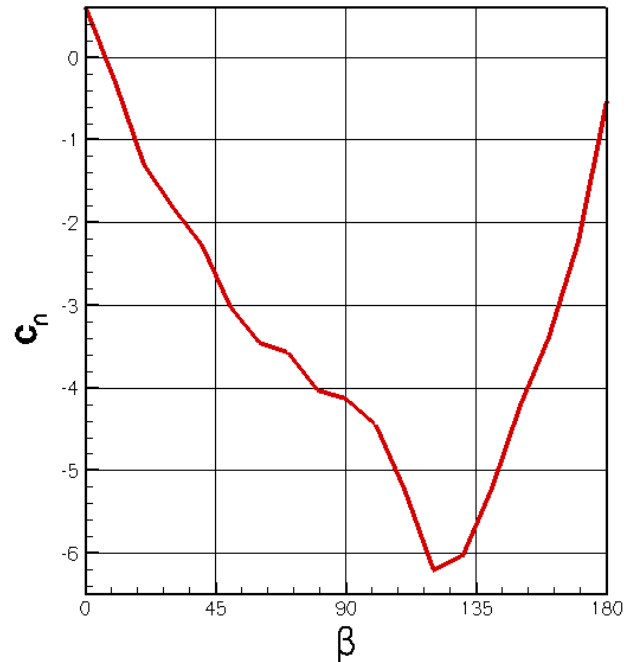


Fig. 7: Yaw moment coefficient as function of angle of yaw ($\alpha=0^\circ$)

3.1.2 Contribution of the empennage system to aerodynamic stability of the fuselage

The empennage consists of the two horizontal and the two vertical stabilizers which are mounted on the tailboom (Fig. 8). The tail rotor mount is an additional vertical stabilizer. The horizontal stabilizers are inverted airfoil sections, which produce a negative lift in forward flight.

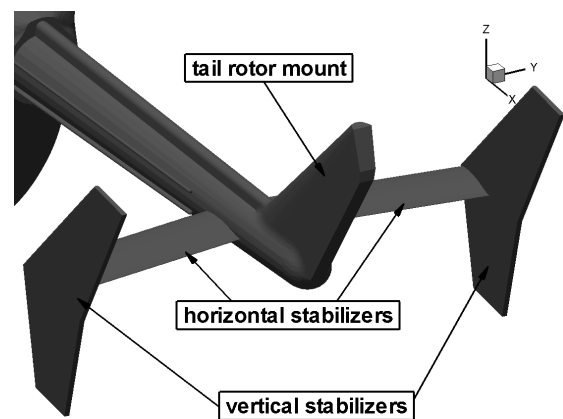


Fig. 8: Empennage at the tailboom of the helicopter

The empennage provides stability in pitch and in yaw. In Fig. 9 the influence of the horizontal stabilizers on the characteristic of the pitching moment as a function of angle of attack can be seen. Without the empennage the fuselage tail configuration produces a pitching moment which acts in the same rotating direction as the pitch-

angle increment. This results in a negative stability derivative in pitch. As can be seen in Fig. 9 the entire configuration with empennage changes the pitching-moment characteristics in such a way that the moment acts opposite to the pitch-angle increment.

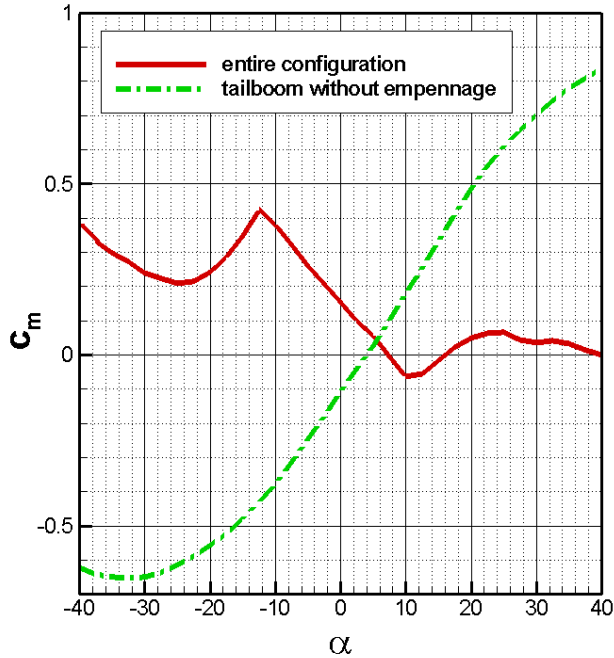


Fig. 9: Pitching moment coefficient as function of angle of attack with and without the empennage ($\beta=0^\circ$)

Besides the horizontal stabilizers the empennage consists of two vertical stabilizers mounted at the tips of the horizontal stabilizers. Fig. 10 shows that the configuration without the empennage also produce a stabilizing moment beyond $\beta=20^\circ$. This moment which acts opposite to the rotation direction is amplified by the vertical stabilizers as shown by the graph of the entire configuration.

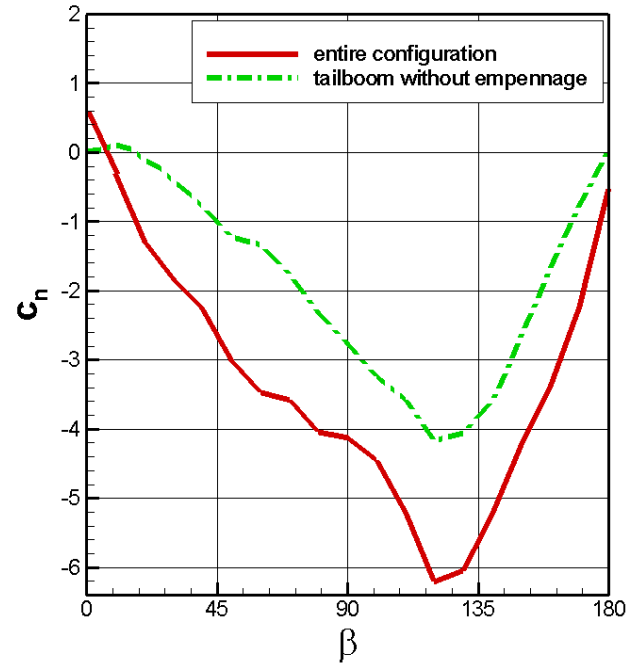


Fig. 10: Yaw moment coefficient as function of angle of attack with and without the empennage ($\alpha=0^\circ$)

3.2 Velocity measurements

Velocity measurements are conducted at a free stream velocity of 25 m/s ($Re_{ref}=0.53 \times 10^6$) and at two angles of attack: $\alpha_1 = 0^\circ$, $\alpha_2 = 25^\circ$. Two different model configurations, with and without rotor hub, were considered. Measurements were taken in a cross-flow plane at a distance of $x/l_{ref}=3.68$ from the origin of the model coordinate system. Due to restrictions of the traversing system, the measured plane is divided into three sub planes. Coordinates and the distances are based on a wind-tunnel fixed coordinate system. Axial velocity and vorticity components point in the x-direction of the coordinate system shown in Fig. 2.

The velocity measurements have been made in the wind-tunnel facility C of the Institute of Aerodynamics (AER) at the Technische Universität München (TUM). The cross section of the wind-tunnel is 1.8×2.7 m. The test section length is 21m. The turbulence level at the nozzle exit is less than 0.5%.

3.2.1 Fuselage and rotor hub wake in forward flight

The fuselage and the rotor hub create a complex wake structure, which includes different kind of vortices. The origins of these vortices are at specific components of the fuselage such as the tip of the engine canopy, the engine outlets and the strong upsweep of the helicopter fuselage. In Fig. 11 the measured cross-flow planes behind the fuselage and the engine canopy are shown. Around the tailboom there is a region with very low axial velocity. This is evidence for a recirculation area. Due to the large upsweep angle of the fuselage-tail the flow can not follow

the geometry and separates beneath the fuselage-tailboom connection. Also the sharp edges of the two engine outlets lead to a separation of the flow at the end of the engine canopy, which can be seen in the corners, close to the tailboom, of the two small measured cross-flow planes.

The influence of the powered rotor hub can be detected in the two smaller measured planes. A larger wake of the rotor hub can be seen on the right plane. Caused by the rotation of the rotor hub, the wake of the rotor mast, swashplate, hub fairing and rods for pitching control of the rotor blades, drifts to the right, which explains the unsymmetrical velocity field in the upper part of the measured plane.

In the lower part of the measuring plane the influence of the strut on the wake can be seen by a region of lower velocity.

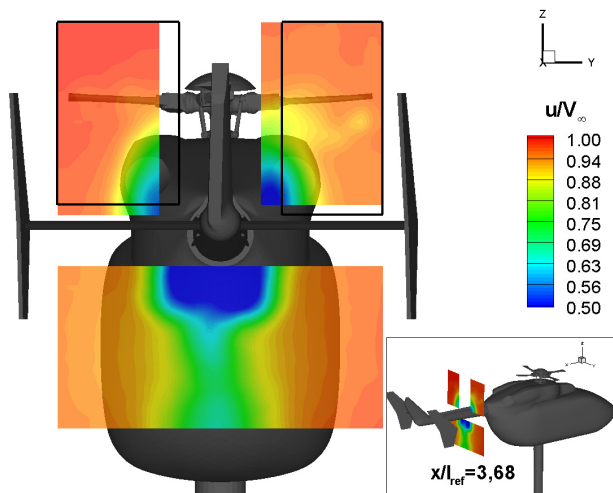


Fig. 11: Axial velocity distribution in the fuselage/rotor hub wake at an angle of attack $\alpha=0^\circ$

The nondimensional axial vorticity distribution of the cross-flow plane at $x/l_{ref}=3.68$ is shown in Fig. 12. Two counter-rotating vortices under the tailboom are the dominant structures in this cross flow section. The origin of these two vortices is a flow separation caused by the strong curvature of the fuselage tail in the upper region, under the tailboom. The separated flow rolls up to a vortex on each side of the separation area. Beneath these two vortices another vortex pair can be seen, which is created by a flow separation on both sides at lower regions of the fuselage tail. The circulation around the tip of the rotor blade segment leads to a vortex with a positive rotation, which can be detected on the right side of the upper right plane. Due to the induced velocity caused by the advancing blade segment the tipvortex moves downwards.

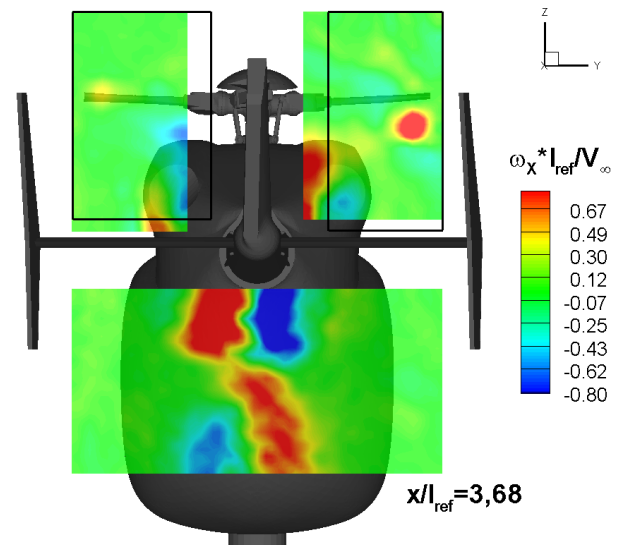


Fig. 12: Axial vorticity distribution in the fuselage/rotor hub wake at an angle of attack $\alpha=0^\circ$

Caused by the sharp edges at the engine outlets the flow separates and builds a counter-rotating vortex pair on each side of the engine canopy, which can be seen near the inner edges of the upper two measured areas. The downwash of the advancing blade also has an effect on these vortices and pushes the right vortex pair more downward than the left one.

3.2.2 Change of the helicopter wake caused by angle of attack variation

The axial velocity distribution of the fuselage/rotor hub wake is shown in Fig. 13. Four areas of low axial velocity can be detected. The upper one has its origin at the engine canopy and rotor hub. Its asymmetric shape can be explained by the rotation of the rotor hub which causes the wake to drift to right section of the measuring plane. An additional separation on the advancing blade segment is also a reason for the larger wake on the right side of the plane. The three lower regions are the wake structures of the two engine outlets and the tailboom.

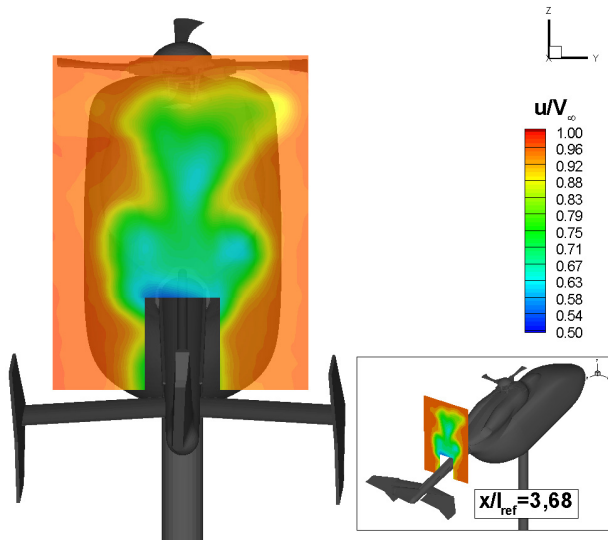


Fig. 13: Axial velocity distribution in the fuselage/rotor hub wake at an angle of attack $\alpha=25^\circ$

In Fig. 14 the axial vorticity is shown on a cross-flow plane in the wake of the configuration with rotor hub at an angle of attack $\alpha=25^\circ$. Compared to the distribution measured at $\alpha=0^\circ$ (Fig. 12), the structure of the wake is quite different. Due to the complex flow around this configuration the origin of the vortices is just a guess and requests more detailed investigation.

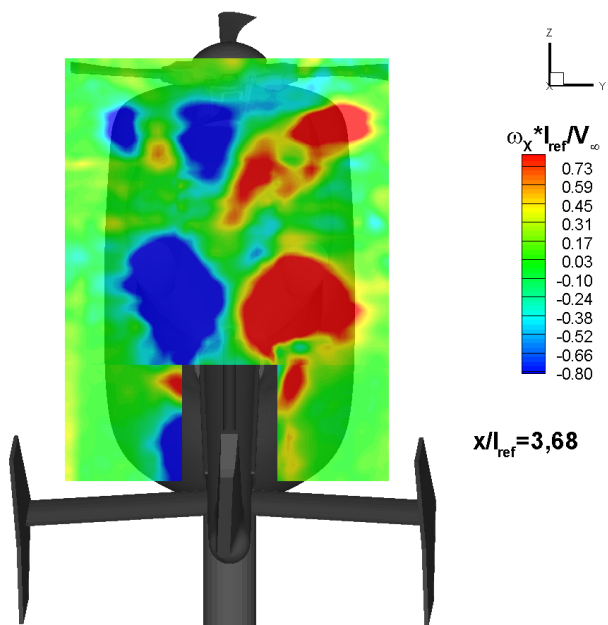


Fig. 14: Axial vorticity distribution in the fuselage/rotor hub wake at an angle of attack $\alpha=25^\circ$

3.2.3 Influence of the rotor hub on the wake

The influence of the powered rotor hub was already shown in the previous sections. Even for the short rotor blade segment, which is cut at a position where the airfoil

section starts, a downwash effect behind and under the advancing blade can be seen. To support that conclusion another measurement without the powered rotor hub was conducted. The results including the axial vorticity can be seen in Fig. 15. Comparing the two distributions it can be seen, that the size of the dominant vortex pair in the lower region of the measured plane with powered rotor hub is larger than without. The position of the vortex cores without rotor hub is lower than with rotor hub.

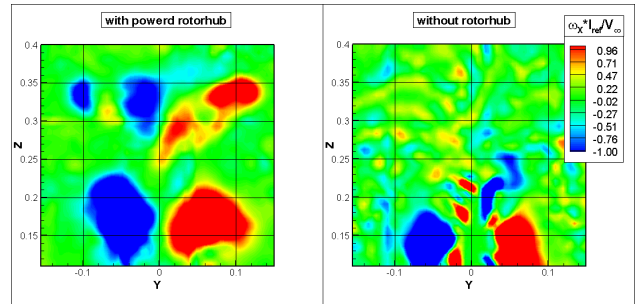


Fig. 15: Comparison of axial vorticity distribution with/without rotor hub at an angle of attack

4. CONCLUSION

The flow around a helicopter fuselage with powered rotor hub has been investigated. For this purpose a 1:7.333 scaled wind-tunnel model was used. Of particular concern were aerodynamic forces and moments over wide angle-of-attack and sideslip ranges. Vorticity and velocity in the helicopter wake have been analyzed. The main results of this study are as follows:

- 1) The helicopter fuselage without empennage has a negative stability derivative in pitch.
- 2) The horizontal stabilizers provide the helicopter with stability in pitch in a specific angle-of-attack range.
- 3) The fuselage-tail configuration has already a stabilizing effect in yaw. This effect is intensified by the vertical stabilizers.
- 4) The separation of flow at the tail of the fuselage causes several vortices in the wake. The wake structure changes with angle-of-attack variation.
- 5) A downwash effect of the rotor hub can be seen by comparing the wake of the configuration with and without rotor hub.

5. FUTURE WORK

The velocity-field measurements in the wake of the fuselage have shown that the wake consists of different kind of vortices. To investigate the formation of the vortex structure and its progress stream downwards, the velocity field in the fuselage wake will be measured by stereo PIV in more detail. For this purpose several planes

behind the fuselage will be measured for different angles of attack.

To define the origins of the vortices a detailed numerical simulation of the flow around the fuselage is necessary.

The isolated fuselage and rotor hub configuration which is used for this investigation does not include the influence of the main rotor wake. Therefore numerical simulations with an actuator disk model are planned.

ACKNOWLEDGMENTS

This research is funded by Eurocopter Deutschland GmbH under the German national project SHANEL-L with grant number 20A0603C.

REFERENCES

1. Leishman J. G. Principles of helicopter aerodynamics, Cambridge University Press, New York, 2006.
 2. Gleize, V., Costes, M., H.Frhr. von Geyr, Kroll, N., Renzoni, P., Amato, M., Kokkalis, A., Mottura, L., Serr, C., Larrey, E., Filippone, A., Fischer, A. Helicopter Fuselage Drag Prediction: State of the art in Europe, AIAA, Paper 2001-0999, Jan. 2001.
 3. Filippone, A. Prediction of aerodynamic forces on a helicopter fuselage, The Aeronautical Journal, March 2007, pp175-184.
 4. Le Chuiton, F., D' Alascio, A., Barakos, G., Steijl, R., Schwamborn, D., Lüdeke, H. Computation of the Helicopter Fuselage Wake with the SST, SAS, DES and XLES Models, Notes on Numerical Fluid Mechanics and Multidisciplinary Design, Vol. 97, 2008.
 5. Martin, P.B., Tung, C., Hassan, A.A., Cerchie, D., Roth, J. Active Flow Control Measurements and CFD on a Transport Helicopter Fuselage.
 6. Hermans, C., Hakkaart, J., Preatoni, G., Mikulla, V., Chery, F., Serr, C. The NH90 helicopter development wind tunnel programme.
-